*73600

NASA TECHNICAL NOTE

NASA TN D-4951

NASA TN D-4951

EFFECT OF RADIUS ON BULGING AND FRACTURE OF THROUGH-CRACKED CYLINDRICAL PRESSURE VESSELS AT CRYOGENIC TEMPERATURES

by Timothy L. Sullivan and William S. Pierce

Lewis Research Center
Cleveland, Ohio

NATIONAL AERONAUTICS AND SPACE ADMINISTRATION • WASHINGTON, D. C. • DECEMBER 1968

23660

ERRATA

NASA Technical Note D-4951

EFFECT OF RADIUS ON BULGING AND FRACTURE OF THROUGH-CRACKED CYLINDRICAL PRESSURE VESSELS AT CRYOGENIC TEMPERATURES

by Timothy L. Sullivan and William S. Pierce

December 1968

Page 5: Equation (5) should read

$$\sigma_{hc} = \frac{K_c}{\left\{\frac{1}{2}\left[\pi a \sec\left(\frac{\pi}{2}\frac{\sigma_{hc}}{\sigma_u}\right)\right]\left(1 + \frac{5\pi}{32}\lambda^2\right)\left(4 - \frac{3 - \nu}{1 + \nu}\right)\right\}^{1/2}}$$

Page 5: Equation (6) should read

$$\sigma_{hc} = \frac{K_{cn}}{\left\{\frac{1}{2}\left[\pi a_o \sec\left(\frac{\pi}{2}\frac{\sigma_{hc}}{\sigma_u}\right)\right]\left(1 + \frac{5\pi}{32}\lambda^2\right)\left(4 - \frac{3 - \nu}{1 + \nu}\right)\right\}^{1/2}}$$

Page 5: The fourth equation should read

$$\lambda^2 = \frac{a_o^2}{rt}\sqrt{12(1 - \nu^2)}$$

Issued 4-28-69

NASA TN D-4951

EFFECT OF RADIUS ON BULGING AND FRACTURE OF THROUGH-CRACKED CYLINDRICAL PRESSURE VESSELS AT CRYOGENIC TEMPERATURES

By Timothy L. Sullivan and William S. Pierce

Lewis Research Center
Cleveland, Ohio

NATIONAL AERONAUTICS AND SPACE ADMINISTRATION

For sale by the Clearinghouse for Federal Scientific and Technical Information
Springfield, Virginia 22151 – CFSTI price $3.00

ABSTRACT

Burst tests of through-cracked, thin-walled cylinders fabricated from Ti-5Al-2.5Sn ELI and 2014-T6 Al were conducted at -320° and -423° F (77 and 20 K). The diameters of the cylinders tested were approximately 6 and 18 in. (15 and 46 cm). The titanium alloy test results showed the pressure bulge coefficient was essentially constant for these two diameters. Comparison of the experimental results with an expression for predicting hoop fracture stress proposed by Eiber showed a good fit with the aluminum alloy data but a poor fit with the titanium alloy data.

EFFECT OF RADIUS ON BULGING AND FRACTURE OF THROUGH-CRACKED CYLINDRICAL PRESSURE VESSELS AT CRYOGENIC TEMPERATURES

by Timothy L. Sullivan and William S. Pierce

Lewis Research Center

SUMMARY

In a previous investigation a dimensional analysis was used to account for the reduction in hoop fracture strength due to bulging at the crack tip in thin-walled, through-cracked cylindrical vessels subject to internal pressure. The derived expression contained an empirical constant, the bulge coefficient. In this investigation the effect of cylinder radius on the bulge coefficient is studied.

Cylinders 6.00 and 18.50 inches (15.2 and 47.0 cm) in diameter with a 0.020-inch (0.051-cm) wall thickness were fabricated from the titanium alloy Ti-5Al-2.5Sn, extra-low-interstitial (ELI) grade. Cylinders 5.62 and 18.26 inches (14.3 and 46.4 cm) in diameter with a 0.060-inch (0.152-cm) wall thickness were machined from 2014-T6 extruded aluminum tubing. Through-cracks ranging in length from 1/8 to 2 inches (0.3 to 5.1 cm) were placed in the cylinder walls. The cylinders were pressurized to failure at -320° and -423° F (77 and 20 K).

The titanium alloy tests showed that the bulge coefficient was essentially constant for the two diameters tested. From this it is concluded that the bulge coefficient is independent of cylinder radius, and the bulge coefficient obtained from scale-model tests can be used to predict the strength of full-size through-cracked cylindrical pressure vessels. The aluminum alloy tests showed a variation in the bulge coefficient for the two different diameters. This variation is probably due to the two different diameters of cylinders coming from two different heats of material.

The experimental data are also compared with an expression for predicting hoop fracture stress from material properties alone, and not requiring the evaluation of an empirical constant. The aluminum alloy data fit the predictions of this expression very well. However, a poor fit was obtained with the titanium alloy data, especially for longer crack lengths.

INTRODUCTION

The presence of through-cracks in thin-walled cylindrical pressure vessels can cause failures at stresses significantly less than the yield strength of the material. This reduction in strength can be particularly severe in materials with relatively high strengths. Many of these materials are commonly used to make containment vessels for cryogenic propellants. To avoid premature failures of pressure vessels in which flaws may be present, the designer must have an understanding of fracture mechanics.

Irwin (ref. 1) has developed a fracture analysis for through-cracked flat sheet loaded in tension. The analysis relates the fracture stress to crack length, sheet width, and a single material parameter, fracture toughness. Although the analysis is elastic, a correction for plasticity at the crack tips can be applied. If the flat-sheet analysis is applied to internally pressurized cylindrical pressure vessels, the predicted failure stresses are greater than those obtained experimentally. This is primarily because the flat-sheet analysis does not account for the increase in stress intensity at the crack tips due to bulging and the bending stresses associated with it.

Anderson and Sullivan (ref. 2) use a dimensional analysis to derive the stress intensity due to bulging. The analysis in reference 2 relates the fracture strength of a cylinder to crack length, cylinder radius, fracture toughness, and an empirical bulge coefficient. The analysis was verified at the Lewis Research Center by testing cylinders which contained longitudinal through-cracks of various lengths, but without varying the diameters of the test vessels. Data obtained by Peters and Kuhn (ref. 3) suggested that the analysis adequately accounted for changes in cylinder radius and wall thickness. However, fracture toughness values required for definitive verification were not available for these data.

In structural testing it is usually desirable to test scale models and be able to apply the results to full-size structures. Therefore, the present program was conducted to verify that the bulge coefficient is not affected by cylinder radius. Cylinders with diameters of 6 and 18.5 inches (15.2 and 47.0 cm) and a wall thickness of 0.020 inch (0.051 cm) were fabricated from the titanium alloy Ti-5Al-2.5Sn, extra-low-interstitial (ELI) grade. Cylinders with diameters of 5.62 and 18.26 inches (14.3 and 46.4 cm) and a wall thickness of 0.060 inch (0.152 cm) were machined from extruded 2014-T6 aluminum tubing. The cylinders, containing longitudinal through-cracks ranging in length from 1/8 to 2 inches (0.3 to 5.1 cm), were pressurized to failure at -320° and -423° F (77 and 20 K). The uniaxial properties of the materials investigated are included. The data are also compared with an equation for predicting the fracture strength of internally pressurized, through-cracked cylinders proposed by Eiber, et al. (ref. 4).

ANALYSIS

Fracture Toughness Calculation

Calculation of fracture toughness values from finite-width center-cracked sheet subjected to uniform tension requires a correction for width effect. The Irwin-Westergaard tangent relation has been commonly used for width effect correction. Paris and Sih (ref. 5) indicate that a more accurate width correction is available from the work of Isida (ref. 6). In the discussion portion of reference 7, C. E. Fedderson points out that the polynomial correction of Isida can be replaced with a very compact secant expression. For crack length to specimen width ratios up to 0.8, the secant expression approximates the Isida polynomial within 0.3 percent.

The fracture toughness values reported herein were calculated using the secant width correction expression as indicated in the following equation:

$$K_c = \sigma_c \sqrt{\pi\bar{a} \sec \frac{\pi\bar{a}}{W}} \tag{1}$$

where K_c is the fracture toughness, σ_c the gross fracture stress, W the specimen width, and $\bar{a}$ the critical half-crack length corrected for plasticity effects. In equation (1),

$$\bar{a} = a + \frac{1}{2\pi} \frac{K_c^2}{\sigma_{ys}^2}$$

where a is the critical half-crack length and σ_{ys} is the 0.2-percent offset yield strength of the material.

While not strictly in accordance with the theory used to develop equation (1), a nominal fracture toughness K_{cn} can be calculated from the initial half-crack length a_o using

$$K_{cn} = \sigma_c \sqrt{\pi\bar{a}_o \sec \frac{\pi\bar{a}_o}{W}} \tag{2}$$

where

$$\bar{a}_o = a_o + \frac{1}{2\pi} \frac{K_{cn}^2}{\sigma_{ys}^2}$$

Nominal fracture toughness is always a conservative estimate of the actual fracture toughness. For long cracks where subcritical crack growth is only a small percentage of the initial crack length, K_{cn} is a reasonably accurate indication of K_c.

Fracture Strength of Through-Cracked Cylinders

If equation (1) or (2) were used to predict the critical hoop fracture stress σ_{hc} for an internally pressurized, through-cracked cylinder after establishing the value of K_c or K_{cn} from flat sheet tests, σ_{hc} could be greatly overestimated. This is because equations (1) and (2) do not take into account the bending stresses at the crack tips due to bulging. In reference 2 a dimensional analysis is used to obtain an expression for σ_{hc} that takes into account pressure bulging. From reference 2,

$$\sigma_{hc} = \frac{K_c}{\sqrt{\pi a + \frac{1}{2} \frac{K_c^2}{\sigma_{yb}^2}\left(1 + C \frac{a}{r}\right)}} \tag{3}$$

where σ_{yb} is the 1 to 2 biaxial yield strength, r the cylinder radius, and C a dimensionless bulge coefficient obtained from cylinder burst tests. Based on initial crack length, the critical hoop fracture stress can be calculated from

$$\sigma_{hc} = \frac{K_{cn}}{\sqrt{\pi a_o + \frac{1}{2} \frac{K_{cn}^2}{\sigma_{yb}^2}\left(1 + C_o \frac{a_o}{r}\right)}} \tag{4}$$

where C_o is the bulge coefficient obtained when a_o and K_{cn} are used. The use of equations (3) and (4) is discussed in the section Use of the Bulge Coefficient in Design.

An equation for predicting hoop fracture stress proposed by Eiber, et al. (ref. 4) has the advantage of having no empirical constant to evaluate from burst tests. For plane stress, the Eiber expression states

$$\sigma_{hc} = \frac{K_c}{\left\{\left[\pi a \sec\left(\frac{\pi}{2} \frac{\sigma_{hc}}{\sigma_u}\right)\right]\left(1 + \frac{5\pi}{32}\lambda^2\right)\left(4 - \frac{3 - \nu}{1 + \nu}\right)\right\}^{1/2}} \tag{5}$$

where σ_u is the biaxial ultimate strength, ν is Poisson's ratio, and

$$\lambda^2 = \frac{a^2}{rt}\sqrt{12(1 - \nu^2)}$$

In the expression for λ, t is the cylinder wall thickness. Based on initial crack length, equation (5) becomes

$$\sigma_{hc} = \frac{K_{cn}}{\left\{\left[\pi a_o \sec\left(\frac{\pi}{2} \frac{\sigma_{hc}}{\sigma_u}\right)\right]\left(1 + \frac{5\pi}{32}\lambda^2\right)\left(4 - \frac{3 - \nu}{1 + \nu}\right)\right\}^{1/2}} \tag{6}$$

In this case,

$$\lambda^2 = \frac{a_o}{rt}\sqrt{12(1 - \nu^2)}$$

EXPERIMENTAL APPARATUS AND PROCEDURE

The Ti-5Al-2.5Sn ELI alloy test specimens were fabricated from sheet nominally 0.020 inch (0.051 cm) thick and from a single heat of material. The sheet was received in the annealed condition. The annealing treatment consisted of heating to 1500° F (1090 K) for 1/2 hour followed by air cooling. The mill analysis provided by the supplier is given in the following table:

Titanium alloy composition, wt %							
Al	Sn	Fe	Mn	C	O	N	H (ppm)
5.5	2.4	0.22	0.03	0.03	0.104	0.010	77

Aluminum alloy test specimens were machined from extruded 2014-T6 Al tubing. The tubing for the larger diameter cylinders had a 17.5-inch (44.5-cm) inside diameter and a 19.0-inch (48.2-cm) outside diameter. The tubes were 56 inches (142 cm) long. The heat of material used to make this tubing is designated as Heat A in this report.

The tubing for the smaller diameter cylinders had a 5.5-inch (14.0-cm) inside diameter and a 6.0-inch (15.2-cm) outside diameter. These tubes were 18 inches (46 cm) long. The material used to make this tubing is designated as Heat B. The chemical analysis of these two heats is given in the following table:

Heat	Aluminum alloy composition, wt %									
	Cu	Fe	Si	Mn	Mg	Zn	Ni	Cr	Ti	Sn
A	4.6	0.44	0.97	0.72	0.38	0.07	-----	0.01	0.03	-----
B	4.3	.36	.80	.73	.40	.06	0.005	.01	.025	0.001

Uniaxial Specimens

The smooth uniaxial properties (0.2-percent offset yield strength, ultimate strength, and elongation) were obtained for the titanium alloy and Heat B of the aluminum alloy using specimens with a test section 1/2 inch (1.3 cm) wide and 2 inches (5.1 cm) long. Smooth specimens for Heat A of the aluminum alloy had a test section 3/8 inch (0.95 cm) wide and $1\frac{3}{4}$ inches (4.4 cm) long. The specimens used to determine fracture toughness were 3 inches (7.6 cm) wide with a through-center crack nominally 1 inch (2.5 cm) long. For the titanium alloy, uniaxial specimens were made with the loading direction both parallel (longitudinal specimens) and perpendicular (transverse specimens) to the direction of rolling. Because of the way the titanium cylinders were fabricated, the longitudinal specimens corresponded to the hoop direction. For the aluminum alloy, only specimens perpendicular to the direction of extrusion (transverse specimens) were made. Here, the transverse specimens corresponded to the hoop direction in the cylinders.

Uniaxial specimens for the larger diameter aluminum tubes (Heat A) were machined directly from the tube wall. Uniaxial specimens for the smaller diameter tubes (Heat B) were machined from flattened tube. The extruded tubing was annealed, slit longitudinally, flattened, and reheat treated to the T6 condition. The nominal thickness of all the aluminum specimens was 0.060 inch (0.152 cm).

For the titanium alloy and Heat A of the aluminum alloy, the fracture toughness specimens were prepared by electrical discharge machining central through-the-thickness slots. The specimens were fatigue cracked by low stress cycling the specimens until cracks of the desired length were obtained. The Heat B aluminum alloy fracture toughness specimens contained machined center notches with no fatigue crack extension. The notch root radius obtained by the machining method was about 0.0002 inch (0.0005 cm).

Uniaxial Tests

Uniaxial tests were conducted at 70°, -320°, and -423° F (294, 77, and 20 K). An extensometer was used to measure strain in the smooth specimen tests. Cryogenic temperatures were obtained by immersing the specimen in either liquid nitrogen (-320° F, 77 K) or liquid hydrogen (-423° F, 20 K). To measure the critical crack length on the fracture toughness specimens tested at cryogenic temperatures, the NASA continuity gage was used. This gage is capable of measuring critical crack length within ±0.01 inch (0.03 cm). A complete description of the operation and use of the continuity gage can be found in reference 8.

Biaxial Specimens

Titanium cylinder fabrication. - The titanium alloy cylinders were fabricated using a single longitudinal butt weld. The hoop direction of the cylinder corresponded to the rolling direction of the sheet. Cylinders 6.0 inches (15.2 cm) in diameter and 18 inches (46 cm) long were welded using a tungsten electrode in an argon-inerted chamber. No filler material was added. Cylinders 18.50 inches (47.0 cm) in diameter and 48 inches (122 cm) long were welded in "open air" using an argon-shielded tungsten electrode. A trailing shield and a backup shield were also used to minimize weld contamination. Again, no filler material was added. Flanges were welded on the ends of both size cylinders. After fabrication the cylinders were stress relieved in vacuum by heating to 1100° F (867 K) for 2 hours and then furnace cooled. The uniaxial titanium alloy specimens were also subjected to this stress relief cycle.

Cracks were placed in the cylinders in a manner similar to that used for the uniaxial specimens. Slots of various lengths were electrical discharge machined through the cylinder wall. The slots were parallel to and 180° from the longitudinal weld. To obtain fatigue cracks the slot was internally patched and the cylinder ends closed by sealing them in heads with a low melting point alloy (see Tank test procedure section, p. 10). The closed cylinders were filled with hydraulic oil and pressure cycled at low stress until fatigue cracks of the desired length were obtained. A volume reducing plug was placed in the larger diameter cylinders to reduce the amount of hydraulic oil required for pressurizing. Initial crack lengths ranged from about 1/4 to 2 inches (0. 63 to 5 cm).

Aluminum cylinder fabrication. - The large and small diameter aluminum alloy cylinders were machined from the corresponding size extruded tubing described earlier. Machining was done alternately on the inside and outside of the rough tubes. This procedure minimized residual stresses and distortion in the cylinder wall. The final wall thickness was nominally 0. 060 inch (0. 152 cm) for both cylinder sizes. The large cylinders had a 18. 26-inch (46. 3-cm) mean diameter and a 48. 0-inch (122-cm) length. The small cylinders were 5. 63 inches (14. 3 cm) in diameter and 18 inches (46 cm) long. A large and a small cylinder are shown in figure 1. Cracks in all the larger cylinders and in the smaller cylinders tested at -423° F (20 K) were prepared in the same manner as those in the titanium alloy cylinders. The smaller aluminum cylinders tested at -320° F (77 K) contained machined through-the-thickness notches. The notch root radius obtained by this method was about 0. 0002 inch (0. 0005 cm). It is believed that the machined notches were sharp enough to simulate fatigue cracks. Initial flaw lengths ranged from 1/8 to 2. 0 inches (0. 32 to 5. 1 cm).

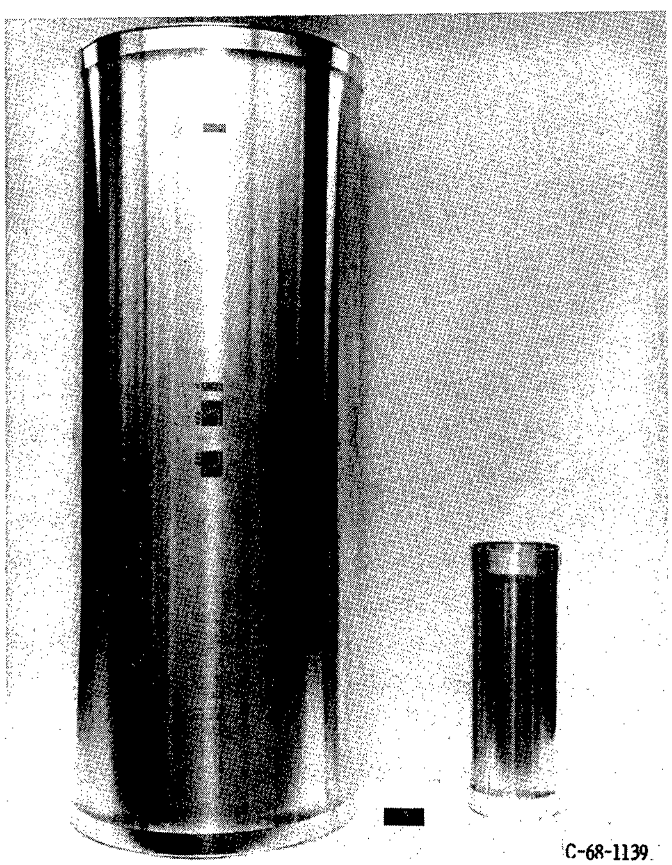

Figure 1. - Aluminum alloy cylindrical pressure vessels.

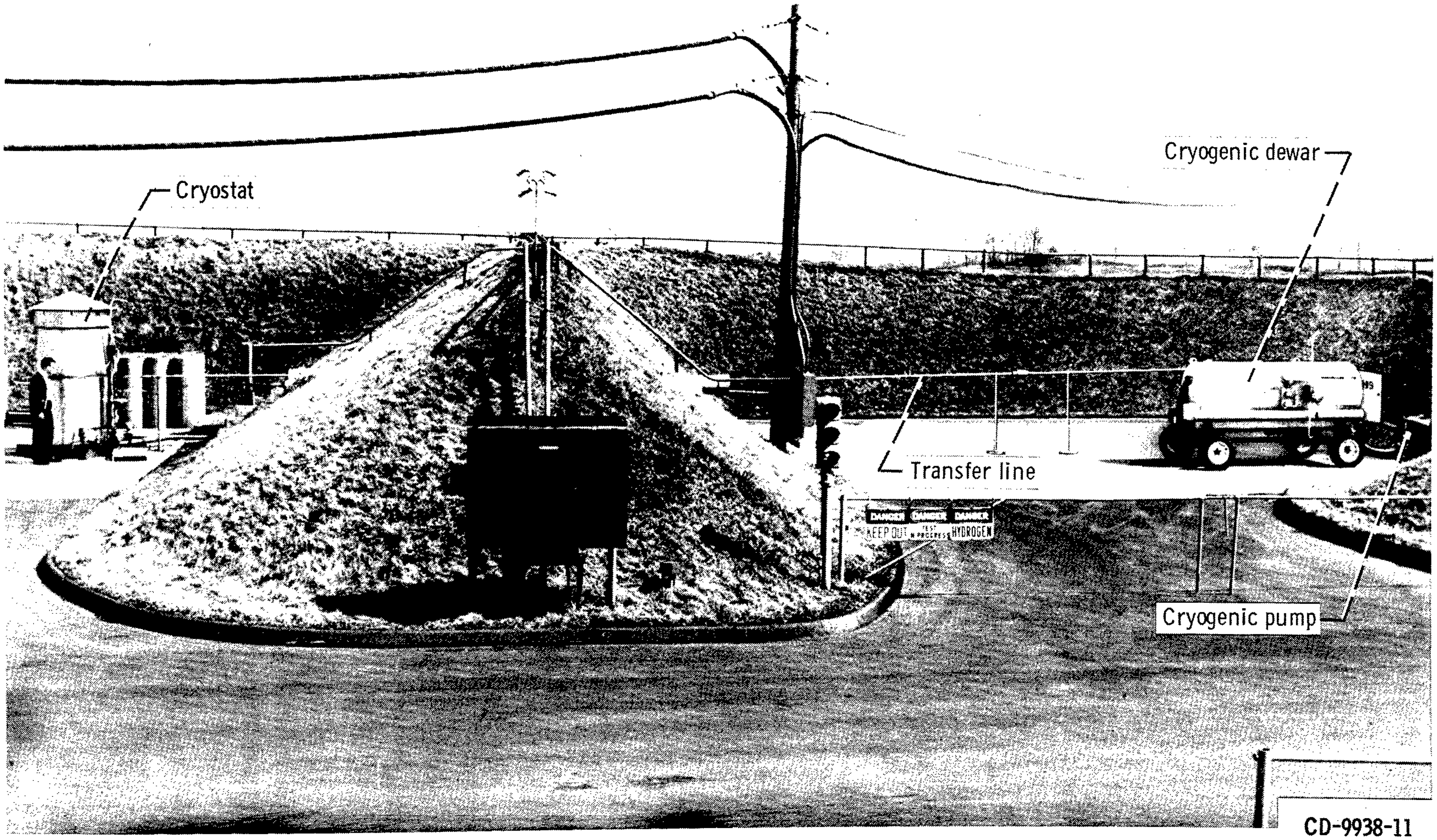

Figure 2. - Facility for bursting 18-inch (46-cm) diameter pressure vessels.

Biaxial Tests

Large diameter tank burst facility. - Figure 2 shows the 18-inch (46-cm) diameter tank burst facility. It consists primarily of a cryostat (an insulated vessel for containing cryogens), a 70-foot (21-m) vacuum-jacketed transfer line, a supply dewar, and a cryogenic liquid pump. The cryostat is a larger version of the one described in reference 9 but does not have a liquid hydrogen shield. The pump is a single-stage positive-displacement unit capable of pumping 2.5 gallons per minute (0.01 m^3/min) at 4000 psi (2760 N/cm^2). A variable speed motor drive was used to power the pump.

Tank test procedure. - Biaxial tests were conducted at -320° and -423° F (77 and 20 K). Cryogenic temperatures were obtained by immersing and filling the test specimen with either liquid nitrogen (-320° F, 77 K) or liquid hydrogen (-423° F, 20 K). The NASA continuity gage was again used to measure the critical crack length.

The cylinder ends were sealed in heads with a low melting point alloy. Reference 10 describes the type of end closures and the test procedure for the small cylinders. The method of patching the flawed area is described in reference 9.

The large specimen assembly contained a filler plug to reduce the volume of pressurized liquid in the system during testing. The specimen was placed inside the cryostat and immersed in the cryogenic liquid. The cryogen was pumped into the bottom of the test vessel and vented through a remotely operated throttling valve. Pressure inside the vessel was increased by slowly throttling the valve until failure occurred.

RESULTS AND DISCUSSION

Uniaxial Results

The uniaxial test results are tabulated in tables I and II. In table I the yield and ultimate strengths are given at 70°, -320°, and -423° F (294, 77, and 20 K). For the titanium alloy, elongation in 2 inches (5 cm) is also included. In table II the results of the fracture toughness tests at -320° and -423° F (77 and 20 K) are given. In most cases three uniaxial specimens were tested at each condition.

Titanium properties. - The average values of yield and ultimate strength, and fracture toughness tabulated in tables I and II for the titanium alloy are plotted in figure 3 as a function of temperature. The averages obtained from longitudinal and transverse specimens are compared. When yield and ultimate strength were considered, only a negligible directionality effect was evident at 70° F (294 K). However, at cryogenic temperatures a slight directionality effect was evident. The maximum effect occurred in the yield strength at -423° F (20 K) where the transverse average was about 4 percent lower than the longitudinal average.

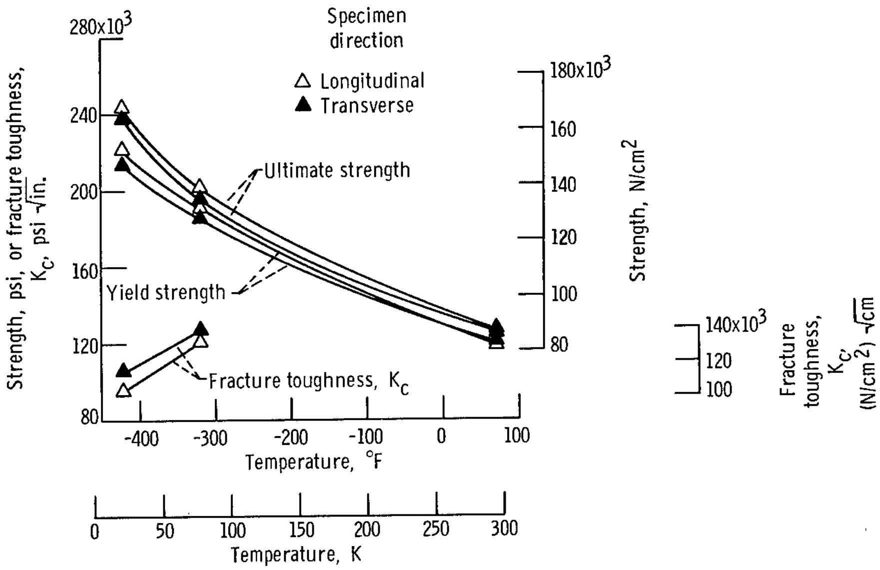

Figure 3. - Average uniaxial mechanical properties of material used to fabricate Ti-5Al-2.5Sn ELI cylinders.

Fracture toughness also exhibited some directionality effect. As would be expected from the lower transverse yield strength, the transverse fracture toughness averages were higher than the longitudinal toughness averages. At -423° F (20 K) the difference was about 10 percent.

Aluminum properties. - The average values of yield strength and ultimate strength, and fracture toughness tabulated in tables I and II for the two heats of the aluminum alloy are plotted in figure 4 as functions of temperature. Only transverse specimens were

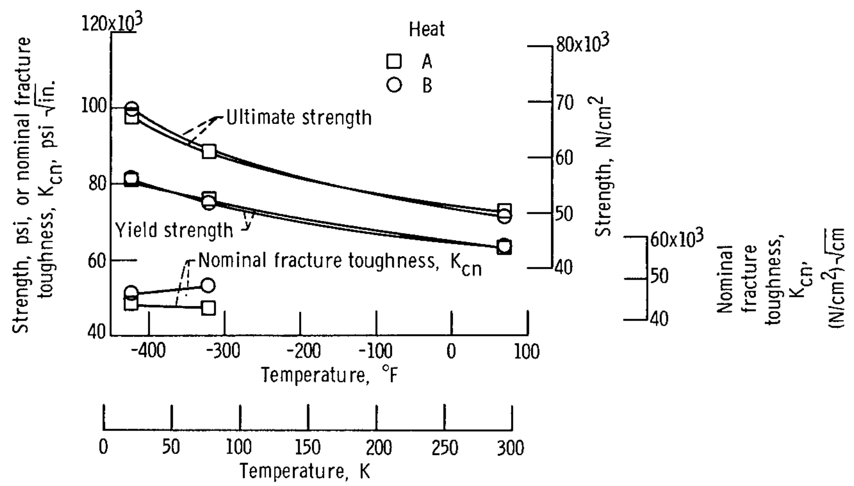

Figure 4. - Comparison of average uniaxial mechanical properties of the two heats of material used to make 2014-T6 aluminum cylinders.

tested. There was a negligible difference in the smooth properties of the two heats. However, at -320° F (77 K) the nominal fracture toughness of Heat A was about 10 percent lower than that of Heat B.

Titanium Cylinder Tests

Biaxial yield strength. - Calculation of the bulge coefficient requires knowledge of the 1 to 2 biaxial yield strength σ_{yb}. For an isotropic material such as the aluminum alloy studied in this investigation, the 1 to 2 biaxial yield strength is assumed to be 1.15 times the uniaxial yield strength. However, sheet of certain titanium alloys, including Ti-5Al-2.5Sn ELI, exhibit anisotropic behavior. This particular form of anisotropy, which is called texturing, can result in 1 to 2 biaxial yield strengths considerably in excess of 15 percent above uniaxial yield strength. In textured titanium sheet the basal planes of the hexagonal-close-packed crystals tend to orient themselves parallel to the plane of the sheet. This crystallographic orientation resists through-thickness deformation and, in biaxial stress field, results in yield strengths that can be considerably greater than the uniaxial yield strength.

To determine the amount of texture strengthening in the titanium alloy studied in this investigation, a single uncracked 6-inch (15.2-cm) diameter cylinder was pressurized to burst at room temperature. A yield strength of 148 000 psi (102 000 N/cm^2) was obtained. This is about a 25-percent increase over uniaxial yield strength. It was shown in reference 11 that the biaxial yield strength of a textured material could be predicted from its plastic Poisson's ratio. Plastic Poisson's ratios were obtained for the titanium alloy at 70°, -320°, and -423° F (294, 77, and 20 K). Based on these values and the actual room temperature biaxial yield strength, the cryogenic biaxial yield strengths were calculated to be 234 000 psi (161 000 N/cm^2) at -320° F (77 K) and 261 000 psi (180 000 N/cm^2) at -423° F (20 K). These values were used in the computation of the bulge coefficient.

Cracked cylinder tests. - The results of the through-cracked titanium alloy cylinder burst tests are tabulated in table III. In figure 5 hoop fracture stress is plotted as a function of crack length.

Hoop fracture strengths obtained at -320° and -423° F (77 and 20 K) are plotted against the initial crack length in figures 5(a) and (b), respectively, and against critical crack length in figures 5(c) and (d), respectively. The results of the 6-inch (15.2-cm) diameter cylinder tests were used to calculate a weighted average of the bulge coefficient C_0 or C. The weighting system used to determine the average is explained in detail in reference 2. This weighted average C_0 (or C) was used to predict the fracture strength of the 18.5-inch (47-cm) diameter cylinders. As can be seen in figures 5(a)

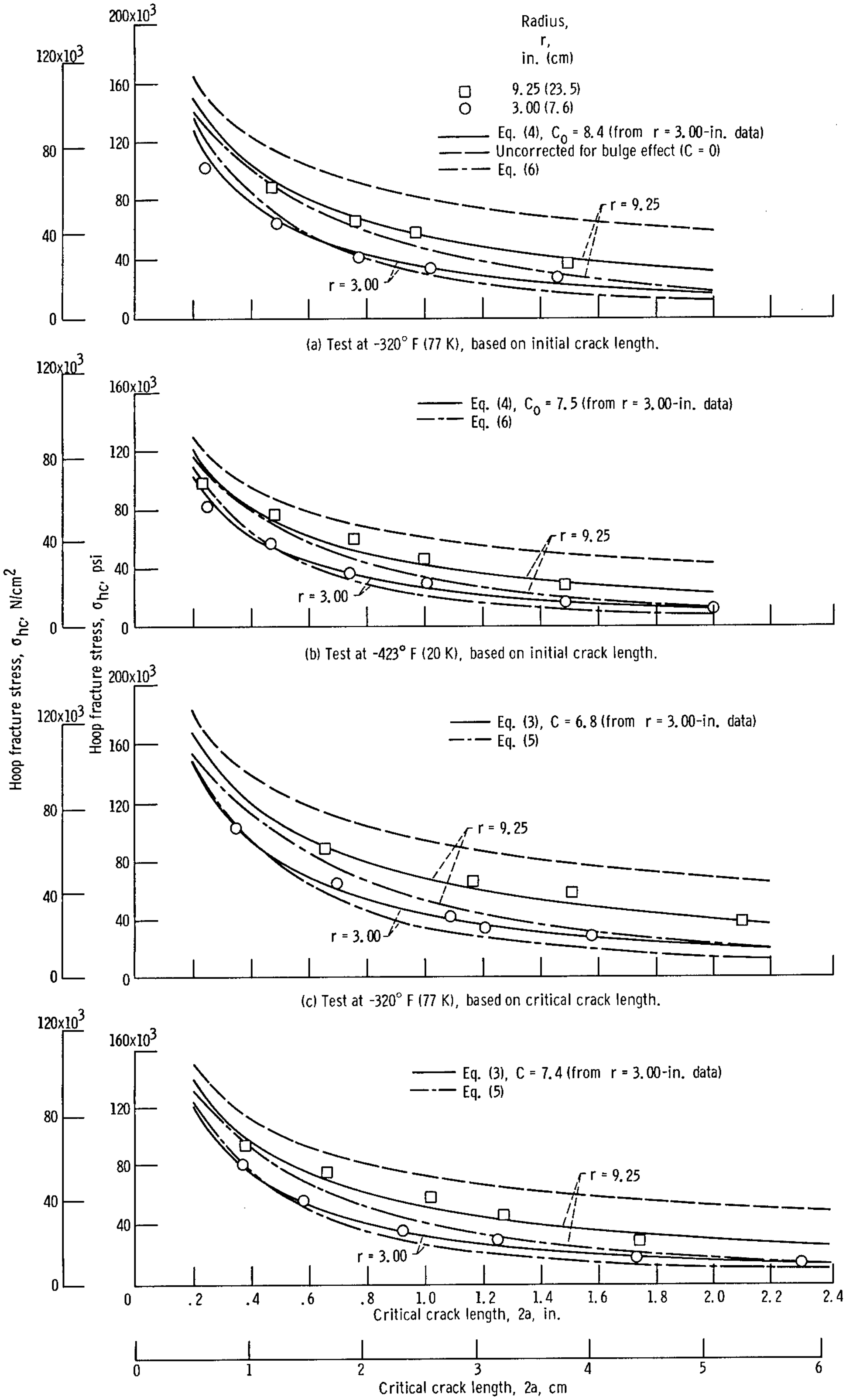

(a) Test at -320° F (77 K), based on initial crack length.

(b) Test at -423° F (20 K), based on initial crack length.

(c) Test at -320° F (77 K), based on critical crack length.

(d) Test at -423° F (20 K), based on critical crack length.

Figure 5. - Strength of cracked Ti-5Al-2.5Sn ELI alloy cylinders.

to (d), the curves predicting the fracture stresses of the larger diameter cylinders are in good agreement with the experimental data.

For the titanium alloy tests little variation was found in the weighted bulge coefficient. This was true even when temperature and diameter were varied independent of whether the analysis was based on initial or critical crack length. A simple average of all the weighted averages tabulated in table III for the titanium alloy gives a value of 7.7. Using this value to predict hoop fracture stress would affect the curves in figure 5(b) and (d) a negligible amount. It would shift the curves in figure 5(a) upward by a nearly constant amount averaging about 1600 psi (1100 N/cm^2) for the 6-inch (15.2-cm) diameter curve and about 1300 psi (900 N/cm^2) for the 18.5-inch (47.0-cm) diameter curve. It would shift the curves in figure 5(c) downward by about 2500 psi (1700 N/cm^2) for the 6-inch (15.2-cm) diameter curve and about 2000 psi (1400 N/cm^2) for the 18.5-inch (47.0-cm) diameter curve.

The preceding discussion should not be interpreted to indicate that the bulge coefficient obtained for a material at one temperature can be applied to another temperature. The consistency of the bulge coefficient obtained with the titanium alloy may be coincidental. Previous tests (ref. 2) have shown a significant effect on the bulge coefficient of temperature and whether it is based on initial or critical crack length. Conservative designs require testing the scale-model cylinders at the same temperature the full-size cylinders will be subjected to.

In each of figures 5(a) to (d) a curve is drawn showing the predicted fracture strength using flat sheet theory (i.e., ignoring the effect of pressure bulging). The figures show that a considerable amount of error is introduced by neglecting the effect of bulging. This is especially true for longer crack lengths. The 18.5-inch (47-cm) diameter cylinders may be considerably smaller than those used in actual aerospace applications. However, going from 6- to 18.5-inch (15.2- to 47-cm) diameter cylinders reduced the loss of strength due to bulging by about one-half. It is quite likely that the bulge coefficient obtained from the 6-inch (15.2-cm) diameter cylinders can be used to accurately predict the fracture strength of full-size through-cracked cylindrical pressure vessels of the same wall thickness.

In figures 5(a) to (d), the hoop fracture stress predicted using the expression proposed by Eiber, et al. (ref. 4) is also shown. The fracture toughness values used in equations (5) and (6) were those obtained from flat-sheet tests (table II). The biaxial ultimate strengths were estimated to be 247 000 psi (170 000 N/cm^2) at -320° F (77 K) and 264 000 psi (182 000 N/cm^2) at -423° F (20 K). Poisson's ratios were estimated to be 0.35 at -320° F (77 K) and 0.34 at -423° F (20 K).

The agreement with the experimental data was not good, especially for longer cracks. Eiber indicates that the applicability of his expression is limited by the value of λ. He reports reasonable results for λ as large as 8.2. The maximum value of λ

attained with the titanium alloy data was about 7.5. The results of the titanium alloy tests would appear to indicate that cylinder wall thickness (or degree of bulging), rather than λ, may limit the applicability of the Eiber expression.

Aluminum Cylinder Tests

The results of the through-cracked aluminum alloy cylinder burst tests are tabulated in table III. In figure 6 hoop fracture stress is plotted as a function of crack (or notch) length. In figures 6(a) and (b), the data are compared in the same manner as described

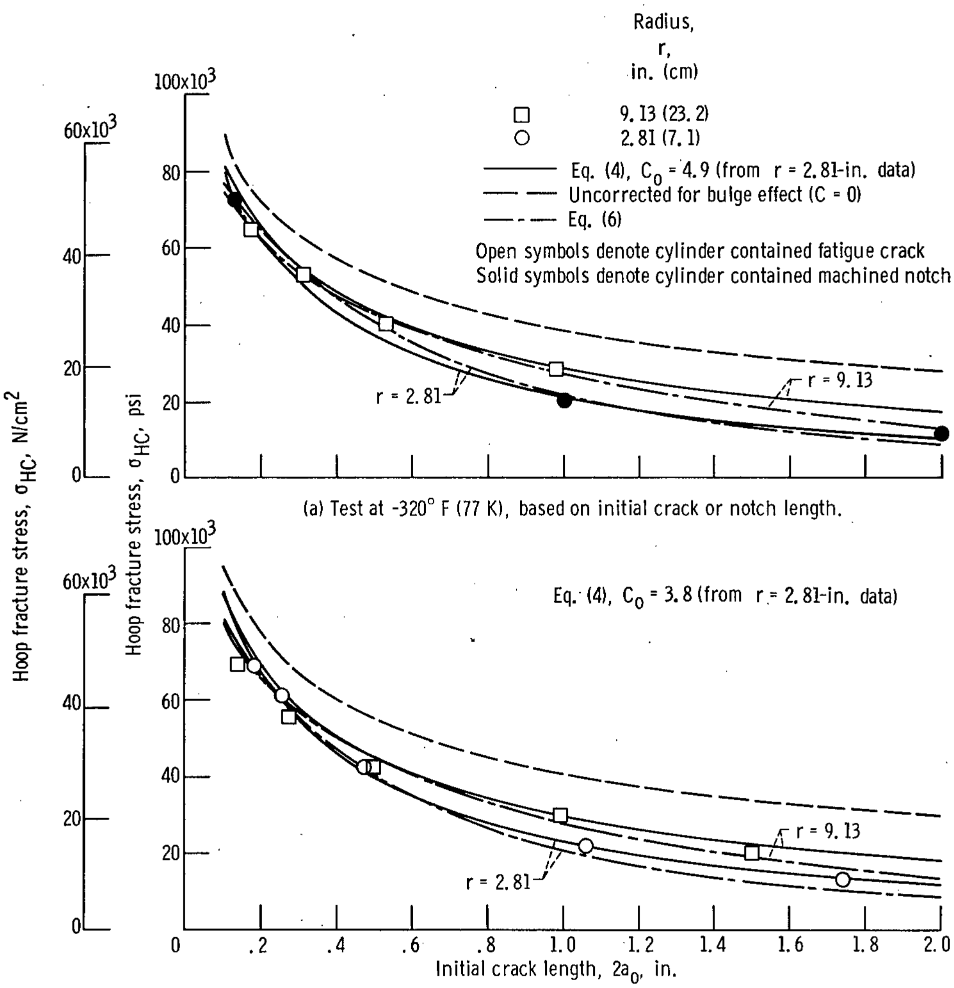

(b) Test at -423° F (20 K), based on initial crack length.

Figure 6. - Strength of 2014-T6 aluminum alloy cylinders.

for the titanium alloy data. The bulge coefficient obtained from the smaller diameter cylinder tests was used to predict the fracture strength of the larger diameter cylinders.

As table III shows, the bulge coefficient obtained from the smaller cylinders was less than that obtained from the tests of the larger cylinders. However, the predicted hoop fracture stress is relatively insensitive to this difference in the bulge coefficient. Therefore, the fracture strengths predicted for the larger cylinders were only slightly greater than those actually obtained in the larger cylinder tests. Had it been possible to obtain both size cylinders from the same heat of material, it is probable that even better agreement would have been obtained. Conclusive results require that materials from the same heat and with the same processing history be compared.

In figures 6(c) and (d) the results of the larger diameter tank tests at -320° and -423° F (77 and 20 K), respectively, are plotted as functions of critical crack length.

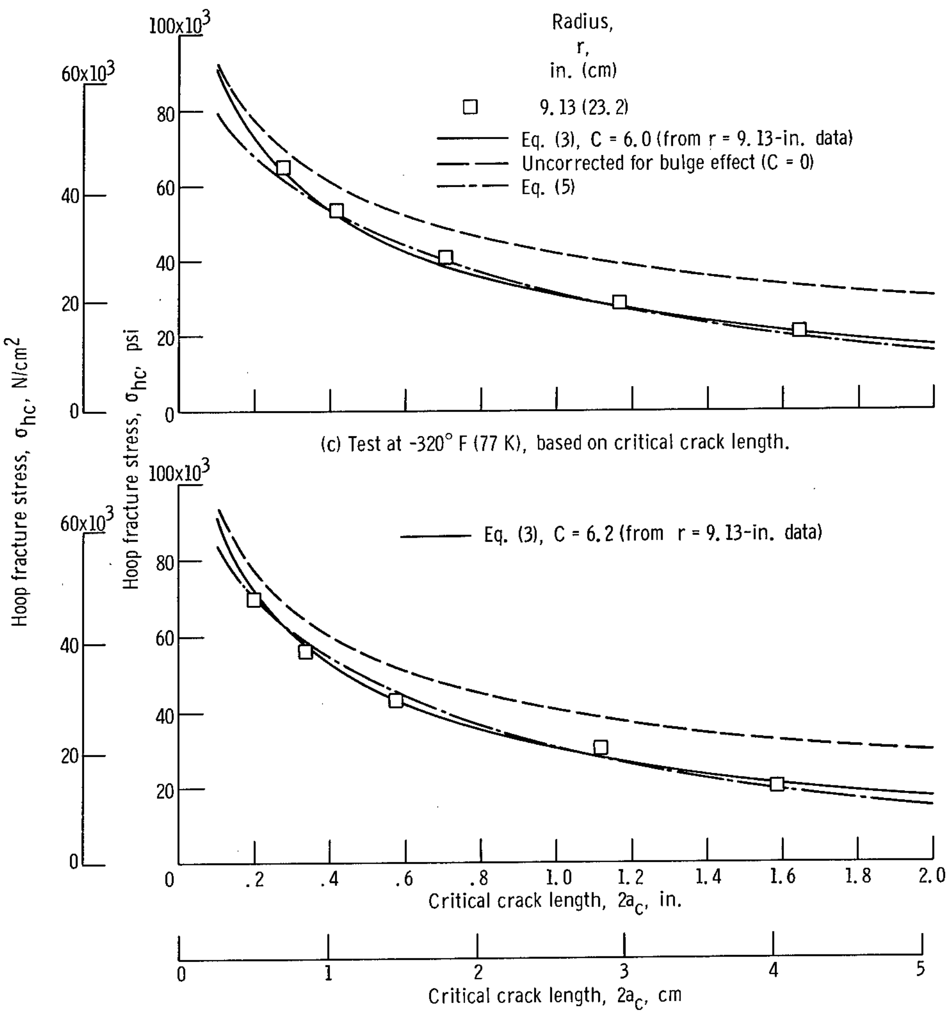

(c) Test at -320° F (77 K), based on critical crack length.

(d) Test at -423° F (20 K), based on critical crack length.

Figure 6. - Concluded.

Because subcritical crack growth was not measured on the smaller cylinders, no comparison to determine scale effect could be made. The weighted average C obtained from the larger diameter cylinder tests was used in equation (3) to obtain the solid curves shown in these two figures.

In figures 6(a) to (d) the hoop fracture stress predicted using the expression proposed by Eiber is again shown. The fracture toughness values used in equations (5) and (6) were obtained from flat-sheet tests (table II). The biaxial ultimate strengths were assumed to be 15 percent greater than uniaxial ultimate strengths. Poisson's ratio was assumed to be 0.33.

For the aluminum alloy, the hoop fracture stress predicted using the Eiber expression was generally in good agreement with the experimental data. In figures 6(a) and (b), it gave a more conservative prediction of σ_{hc} for the larger diameter cylinders than did the bulge coefficient expression. In figures 6(c) and (d), σ_{hc} predicted from both expressions fit the data very well.

Use of the Bulge Coefficient in Design

From the viewpoint of the designer, the curves based on initial crack length would be of greater value than those based on critical crack length. The designer may have no knowledge of the amount of subcritical crack growth to expect. From tests of scale-model through-cracked cylinders he could obtain a bulge coefficient C_0 for his particular application. Burst tests of three or four cylinders should be made with through cracks ranging in length from about 1/2 to 2 inches (1.2 to 5.1 cm). In all cases the crack must be long enough so that the hoop fracture stress does not exceed 80 percent of the yield strength. A curve of σ_{hc} against $2a_0$ could be drawn for the diameter of the cylinder being considered by using an average C_0 obtained from the burst tests. From this curve the designer could (1) for a given design stress, determine the maximum length through-crack the cylinder could tolerate, and (2) from the length of a through-crack in an existing cylinder, determine the cylinder fracture stress. However, for short cracks, where subcritical crack growth can be a large percentage of initial crack length, special care must be taken. (See the tabulated values of C_0 and C in table III.) In this case, neglecting subcritical crack growth could lead to unconservative results.

CONCLUDING REMARKS

Test results of cylinders fabricated from 0.020-inch (0.051-cm) thick sheet of the titanium alloy Ti-5Al-2.5Sn ELI showed that when the cylinder diameter was increased from 6.00 to 18.50 inches (15.2 to 47.0 cm) the bulge coefficient remained essentially constant. It is reasonable to believe that tests of larger diameter cylinders would result in no change in the value of the bulge coefficient obtained. It is concluded that the bulge coefficient is independent of cylinder diameter. Therefore, tests of scale-model cylinders can be used to accurately predict the fracture strength of full-size, through-cracked cylindrical pressure vessels of the same wall thickness.

Test results of 5.62- and 18.26-inch (14.3- and 46.4-cm) diameter, 0.060-inch (0.152-cm) wall cylinders machined from 2014-T6 extruded aluminum tubing showed a variation in the bulge coefficient. This variation was probably due to the fact that the two different diameter cylinders came from two heats of material. However, use of the bulge coefficient obtained from the smaller diameter cylinders resulted in predicted hoop fracture stresses for the larger diameter cylinders only slightly higher than those obtained experimentally.

The experimental results were compared with an expression for predicting hoop fracture stress of through-cracked, cylindrical pressure vessels proposed by Eiber. The aluminum alloy data fit the predictions of this expression very well while the titanium alloy data did not. The Eiber expression may not be applicable to cylinders with walls so thin that the bulge effect is very pronounced.

Lewis Research Center,
National Aeronautics and Space Administration,
Cleveland, Ohio, August 29, 1968,
124-08-08-19-22.

REFERENCES

1. ASTM Special Committee on Fracture Toughness Testing of High-Strength Metallic Materials: Fracture Testing of High-Strength Sheet Materials. Part I. ASTM Bull. No. 243, Jan. 1960, pp. 29-40.

2. Anderson, Robert B.; and Sullivan, Timothy L.: Fracture Mechanics of Through-Cracked Cylindrical Pressure Vessels. NASA TN D-3252, 1966.

3. Peters, Roger W.; and Kuhn, Paul: Bursting Strength of Unstiffened Pressure Cylinders with Slits. NACA TN 3993, 1957.

4. Eiber, R. J.; Maxey, W. A.; Duffy, A. R.; and McClure, G. M.: Behavior of Through-Wall and Surface Flaws in Cylindrical Vessels. Paper presented at the National Symposium on Fracture Mechanics, Lehigh Univ., Bethlehem, Pa., June 17-19, 1968.

5. Paris, Paul C.; and Sih, George C.: Stress Analysis of Cracks. Fracture Toughness Testing and Its Applications. Spec. Tech. Publ. No. 381, ASTM, 1965, pp. 30-83.

6. Isida, Makoto; and Itagaki, Yoshio: Stress Concentration at the Tip of a Central Transverse Crack in a Stiffened Plate Subjected to Tension. Proceedings of the Fourth U. S. National Congress of Applied Mechanics. Vol. 2. R. M. Rosenberg, ed., ASME, 1962, pp. 955-969.

7. Brown, William F., Jr.; and Srawley, John E.: Plane Strain Crack Toughness Testing of High Strength Metallic Materials. Spec. Tech. Publ. No. 410, ASTM, 1967, p. 77.

8. Sullivan, Timothy L.; and Orange, Thomas W.: Continuity Gage Measurement of Crack Growth on Flat and Curved Surfaces at Cryogenic Temperatures. NASA TN D-3747, 1966.

9. Getz, David F.; Pierce, William S.; and Calvert, Howard F.: Correlation of Uniaxial Notch Tensile Data with Pressure-Vessel Fracture Characteristics. Paper No. 63-WA-187, ASME, 1963.

10. Calvert, Howard F.; and Kemp, Richard H.: Determination of Pressure Vessel Strengths at -423° F as Influenced by Notches of Various Radii. Paper No. 520B, SAE, Apr. 1962.

11. Sullivan, Timothy L.: Texture Strengthening and Fracture Toughness of Titanium Alloy Sheet at Room and Cryogenic Temperatures. NASA TN D-4444, 1968.

TABLE I. - UNIAXIAL SMOOTH PROPERTIES

(a) U. S. Customary Units

Temperature, °F	0.2-Percent yield strength, psi	Ultimate strength, psi	Elongation in 2 in., percent	0.2-Percent yield strength, psi	Ultimate strength, psi	Elongation in 2 in., percent
Ti-5Al-2.5 Sn ELI						
	Longitudinal properties			Transverse properties		
70	121×10^3	128×10^3	14.5	119×10^3	125×10^3	12.0
	118	125	12.0	123	128	12.5
	117	126	13.0	120	124	14.5
Average	119×10^3	126×10^3	13.2	121×10^3	126×10^3	13.0
-320	191×10^3	202×10^3	15.5	184×10^3	196×10^3	20.0
	190	199	15.0	188	197	15.5
	192	201	14.5	184	194	13.5
Average	191×10^3	201×10^3	15.0	185×10^3	196×10^3	16.3
-423	224×10^3	244×10^3	12.5	215×10^3	239×10^3	13.0
	220	242	Specimen shattered	213	239	14.5
	221	244	10.5	213	237	10.0
Average	221×10^3	243×10^3	11.5	214×10^3	238×10^3	12.5
2014-T6 Al						
	Heat A (18.26-in. cylinders)			Heat B (5.62-in. cylinders)		
70	64.0×10^3	73.1×10^3	----	63.6×10^3	71.9×10^3	----
	62.8	72.3	----	63.4	71.4	----
	62.6	72.0	----	63.0	71.2	----
Average	63.1×10^3	72.5×10^3	----	63.3×10^3	71.5×10^3	----
-320	75.6×10^3	88.9×10^3	----	75.0×10^3	--------	----
	74.9	87.7	----	--------	--------	----
	75.7	88.0	----	--------	--------	----
Average	75.4×10^3	88.2×10^3	----	75.0×10^3	--------	----
-423	80.5×10^3	97.5×10^3	----	79.9×10^3	97.2×10^3	----
	79.8	97.1	----	82.2	101	----
	--------	--------	----	82.8	101	----
Average	80.2×10^3	97.3×10^3	----	81.6×10^3	99.7×10^3	----

TABLE I. - Concluded. UNIAXIAL SMOOTH PROPERTIES

(b) SI Units

Temperature, K	0.2-Percent yield strength, N/cm^2	Ultimate strength, N/cm^2	Elongation in 5 cm, percent	0.2-Percent yield strength, N/cm^2	Ultimate strength, N/cm^2	Elongation in 5 cm, percent
Ti-5Al-2.5 Sn ELI						
	Longitudinal properties			Transverse properties		
294	83.2×10^3	88.3×10^3	14.5	82.0×10^3	86.3×10^3	12.0
	81.4	86.3	12.0	84.9	87.9	12.5
	80.9	86.9	13.0	82.8	85.5	14.5
Average	81.9×10^3	87.2×10^3	13.2	83.2×10^3	86.5×10^3	13.0
77	132×10^3	139×10^3	15.5	127×10^3	135×10^3	20.0
	131	137	15.0	129	136	15.5
	133	139	14.5	127	134	13.5
Average	132×10^3	138×10^3	15.0	128×10^3	135×10^3	16.3
20	154×10^3	168×10^3	12.5	148×10^3	165×10^3	13.0
	151	167	Specimen shattered	147	165	14.5
	152	168	10.5	147	163	10.0
Average	152×10^3	168×10^3	11.5	147×10^3	164×10^3	12.5
2014-T6 Al						
	Heat A (46.4-cm cylinders)			Heat B (14.3-cm cylinders)		
294	44.1×10^3	50.4×10^3	----	43.8×10^3	49.5×10^3	----
	43.3	49.8	----	43.7	49.2	----
	43.1	49.6	----	43.4	49.1	----
Average	43.5×10^3	50.0×10^3	----	43.6×10^3	49.3×10^3	----
77	52.1×10^3	61.3×10^3	----	51.7×10^3	--------	----
	51.6	60.4	----	--------	--------	----
	52.2	60.6	----	--------	--------	----
Average	52.0×10^3	60.8×10^3	----	51.7×10^3	--------	----
20	55.5×10^3	67.2×10^3	----	55.1×10^3	67.0×10^3	----
	55.0	66.9	----	56.6	69.6	----
	--------	--------	----	57.0	69.6	----
Average	55.3×10^3	67.0×10^3	----	56.2×10^3	68.7×10^3	----

TABLE II. - UNIAXIAL PROPERTIES OF CRACKED (OR NOTCHED) SPECIMENS[a]

(a) U. S. Customary Units

Temperature, °F	Direction (b)	Initial crack length, in.	Critical crack length, in.	Gross fracture stress, psi	Nominal fracture toughness, psi $\sqrt{in.}$	Fracture toughness, psi $\sqrt{in.}$
Ti-5Al-2.5 Sn ELI						
70	L	1.09	(c)	72.5×10^3	---------	---------
		1.02	↓	75.1	---------	---------
	T	1.05	↓	74.0	---------	---------
		1.05	↓	75.0	---------	---------
-320	L	1.04	1.24	74.2×10^3	110×10^3	127×10^3
		1.01	1.21	73.1	106	122
		1.01	1.20	70.2	101	115
	Average	----	----	--------	105×10^3	121×10^3
	T	1.01	1.26	76.3×10^3	111×10^3	133×10^3
		1.04	1.35	70.0	103	128
		1.09	1.28	69.1	105	119
	Average	----	----	--------	106×10^3	127×10^3
-423	L	1.00	1.22	55.2×10^3	76.2×10^3	88.0×10^3
		1.03	1.35	56.9	80.3	98.8
		1.01	1.34	57.3	79.9	99.0
	Average	----	----	--------	78.8×10^3	95.3×10^3
	T	1.04	1.36	62.3×10^3	89.0×10^3	110×10^3
		1.03	1.36	56.7	80.0	99.1
		1.04	1.35	60.5	86.3	106
	Average	----	----	----	85.1×10^3	105×10^3

Temperature, °F	Heat (d)	Initial notch length, in.	Critical crack length, in.	Gross fracture stress, psi	Nominal fracture toughness, psi $\sqrt{in.}$	Fracture toughness, psi $\sqrt{in.}$
2014-T6 Al						
-320	B	0.996	1.27	38.1×10^3	57.5×10^3	72.1×10^3
		1.000	1.40	33.2	48.7	66.3
	Average	-----	----	35.7×10^3	53.1×10^3	69.2×10^3
	A	0.989	1.21	32.2×10^3	46.5×10^3	54.8×10^3
		1.002	1.19	31.9	46.5	53.0
		1.004	1.23	32.6	47.6	56.1
	Average	-----	----	32.2×10^3	46.9×10^3	54.7×10^3
-423	B	1.004	1.15	34.3×10^3	50.0×10^3	55.5×10^3
		1.000	1.15	35.6	52.0	58.0
	Average	-----	----	34.5×10^3	51.0×10^3	56.8×10^3
	A	0.992	1.11	33.6×10^3	48.5×10^3	52.8×10^3
		1.000	1.13	33.6	48.7	53.6
		1.006	1.15	33.0	48.0	53.3
	Average	-----	----	33.4×10^3	48.4×10^3	53.2×10^3

[a]Plates to prevent out-of-plane buckling of crack edges were used on the titanium alloy specimens. Plates were not required on the aluminum alloy specimens.
[b]L, Longitudinal; T, transverse.
[c]Not measured.
[d]Heat A, 18.26-in.-diam. cylinders; Heat B, 5.63-in.-diam. cylinders.

TABLE II. - Concluded. UNIAXIAL PROPERTIES OF CRACKED (OR NOTCHED) SPECIMENS[a]

(b) SI Units

Temperature, K	Direction (b)	Initial crack length, cm	Critical crack length, cm	Gross fracture stress, N/cm^2	Nominal fracture toughness, $(N/cm^2)\sqrt{cm}$	Fracture toughness, $(N/cm^2)\sqrt{cm}$
Ti-5Al-2.5 Sn ELI						
294	L	2.77	(c)	50.0×10^3	---------	---------
		2.59	↓	51.7	---------	---------
	T	2.67	↓	51.0	---------	---------
		2.67	↓	51.7	---------	---------
77	L	2.64	3.15	51.1×10^3	121×10^3	139×10^3
		2.57	3.07	50.4	116	134
		2.57	3.05	48.4	111	127
	Average	----	----	--------	116×10^3	133×10^3
	T	2.57	3.20	52.6×10^3	122×10^3	146×10^3
		2.64	3.43	48.2	113	140
		2.77	3.25	47.6	115	131
	Average	----	----	--------	117×10^3	139×10^3
20	L	2.54	3.10	38.0×10^3	83.7×10^3	96.7×10^3
		2.62	3.43	39.2	88.2	109
		2.57	3.40	39.5	87.8	109
	Average	----	----	--------	86.6	105×10^3
	T	2.64	3.45	42.9×10^3	97.8×10^3	121×10^3
		2.62	3.45	39.1	87.9	109
		2.64	3.43	41.7	94.8	116
	Average	----	----	--------	93.5×10^3	115×10^3

Temperature, K	Heat (d)	Initial notch length, cm	Critical crack length, cm	Gross fracture stress, N/cm^2	Nominal fracture toughness, $(N/cm^2)\sqrt{cm}$	Fracture toughness, $(N/cm^2)\sqrt{cm}$
2014-T6 Al						
77	B	2.53	3.22	26.3×10^3	63.2×10^3	78.3×10^3
		2.54	3.56	22.9	53.5	72.9
	Average	----	----	24.6×10^3	58.4×10^3	76.0×10^3
	A	2.51	3.07	22.2×10^3	51.1×10^3	60.2×10^3
		2.54	3.02	22.0	51.1	58.2
		2.54	3.12	22.5	52.3	61.7
	Average	----	----	22.2×10^3	51.5×10^3	60.1×10^3
20	B	2.55	2.92	23.6×10^3	55.0×10^3	61.0×10^3
		2.54	2.92	24.5	57.1	63.8
	Average	----	----	23.8×10^3	56.1×10^3	62.5×10^3
	A	2.51	2.82	23.2×10^3	53.3×10^3	58.0×10^3
		2.54	2.87	23.2	53.5	58.9
		2.57	2.92	22.7	52.8	58.6
	Average	----	----	23.0×10^3	53.2×10^3	58.5×10^3

[a]Plates to prevent out-of-plane buckling of crack edges were used on the titanium alloy specimens. Plates were not required on the aluminum alloy specimens.

[b]L, Longitudinal; T, transverse.

[c]Not measured.

[d]Heat A, 18.26-in.-diam. cylinders; Heat B, 5.63-in.-diam. cylinders.

TABLE III. - CYLINDER BURST TEST DATA

(a) U. S. Customary Units

Temperature, °F	Cylinder radius, r, in.	Initial crack length, $2a_o$, in.	Critical crack length, 2a, in.	Critical hoop fracture stress, σ_{hc}, psi	Bulge coefficient based on $2a_o$, C_o	Weighted average of C_o	Bulge coefficient based on 2a, C	Weighted average of C
				Ti-5Al-2.5 Sn ELI				
-320	3.00	0.238	0.35	102×10^3	12.50	8.4	7.41	6.8
		.490	.70	63.9	9.39		6.04	
		.774	1.09	41.1	9.57		6.42	
		1.022	1.21	32.9	8.53		7.83	
		1.458	1.58	27.3	6.16		6.61	
	9.25	0.472	0.66	88.0×10^3	11.94	10.0	7.60	5.8
		.762	1.17	64.9	10.32		5.18	
		.968	1.51	57.5	8.40		4.40	
		1.494	2.10	36.6	10.41		6.91	
-423	3.00	0.252	0.37	83.2×10^3	10.13	7.5	6.86	7.4
		.470	.58	57.7	6.93		6.93	
		.740	.92	37.0	7.60		7.14	
		1.008	1.25	30.1	6.26		5.87	
		1.490	1.73	17.0	8.06		8.18	
		1.998	2.30	12.4	7.69		7.84	
	9.25	0.236	0.38	96.0×10^3	21.34	7.8	10.64	7.7
		.484	.66	77.0	5.35		5.00	
		.760	1.02	59.6	4.57		4.31	
		.998	1.27	46.5	6.20		6.23	
		1.486	1.74	28.8	9.63		10.39	
				2014-T6 Al				
-320	2.81	[a]0.125	(b)	72.9×10^3	7.63	4.9	-----	---
		[a]1.000	(b)	20.4	5.41		-----	
		[a]2.000	(b)	11.5	4.30		-----	
	9.13	0.157	0.27	64.7×10^3	17.81	5.9	4.37	6.0
		.310	.42	53.1	6.47		4.97	
		.527	.70	40.5	5.96		4.78	
		.978	1.17	28.3	5.18		5.58	
		1.478	1.64	20.5	5.64		6.66	
-423	2.81	0.182	(b)	68.8×10^3	3.88	3.8	-----	---
		.258	↓	61.2	2.63		-----	
		.474	↓	42.7	3.14		-----	
		1.062	↓	22.0	3.82		-----	
		1.740	↓	13.2	4.13		-----	
	9.13	0.138	0.20	69.2×10^3	23.10	6.2	10.83	6.2
		.274	.33	55.9	9.91		8.11	
		.498	.57	43.0	6.36		6.27	
		.995	1.12	30.1	4.26		4.51	
		1.500	1.58	20.3	6.21		7.01	

[a]Initial notch length.
[b]Not measured.

TABLE III. - Concluded. CYLINDER BURST TEST DATA

(b) SI Units

Temperature, K	Cylinder radius, r, cm	Initial crack length, $2a_o$, cm	Critical crack length, 2a, cm	Critical hoop fracture stress, σ_{hc}, N/cm^2	Bulge coefficient based on $2a_o$, C_o	Weighted average of C_o	Bulge coefficient based on 2a, C	Weighted average of C
Ti-5Al-2.5 Sn ELI								
77	7.62	0.605	0.89	70.4×10^3	12.50	8.4	7.41	6.8
		1.245	1.78	44.0	9.39		6.04	
		1.966	2.77	28.3	9.57		6.42	
		2.596	3.07	22.7	8.53		7.83	
		3.703	4.01	18.8	6.16		6.61	
	23.50	1.199	1.68	60.6×10^3	11.94	10.0	7.60	5.8
		1.935	2.97	44.7	10.32		5.18	
		2.459	3.84	39.6	8.40		4.40	
		3.795	5.33	25.2	10.41		6.91	
20	7.62	0.640	0.94	57.3×10^3	10.13	7.5	6.86	7.4
		1.194	1.47	39.8	6.93		6.93	
		1.880	2.34	25.5	7.60		7.14	
		2.560	3.18	20.7	6.26		5.87	
		3.785	4.39	11.7	8.06		8.18	
		5.075	5.84	8.54	7.69		7.84	
	23.50	0.599	0.97	66.1×10^3	21.34	7.8	10.64	7.7
		1.229	1.68	53.1	5.35		5.00	
		1.930	2.59	41.1	4.57		4.31	
		2.535	3.23	32.0	6.20		6.23	
		3.774	4.42	19.8	9.63		10.39	
2014-T6 Al								
77	7.14	[a]0.318	(b)	48.9×10^3	7.63	4.9	-----	---
		[a]2.540	(b)	14.1	5.41		-----	
		[a]5.080	(b)	7.9	4.30		-----	
	23.2	0.399	0.69	44.6×10^3	17.81	5.9	4.37	6.0
		.787	1.07	36.6	6.47		4.97	
		1.339	1.78	27.9	5.96		4.78	
		2.484	2.97	19.5	5.18		5.58	
		3.754	4.17	14.1	5.64		6.66	
20	7.14	0.462	(b)	47.4×10^3	3.88	3.8	-----	---
		.655	↓	42.2	2.63		-----	
		1.204	↓	29.4	3.14		-----	
		2.697	↓	15.2	3.82		-----	
		4.420	↓	9.1	4.13		-----	
	23.2	0.351	0.51	47.7×10^3	23.10	6.2	10.83	6.2
		.696	.84	38.5	9.91		8.11	
		1.265	1.45	29.6	6.36		6.27	
		2.527	2.85	20.7	4.26		4.51	
		3.810	4.01	14.0	6.21		7.01	

[a]Initial notch length.

[b]Not measured.